

A Novel Bitwise Factor Graph Belief Propagation Detection Algorithm for Massive MIMO System

Lin Li^{1,2} and Weixiao Meng^{1,2}(✉)

¹ Communications Research Center, Harbin Institute of Technology, Harbin, China

² Key Laboratory of Police Wireless Digital Communication,
Ministry of Public Security, Harbin, China
wxmeng@hit.edu.cn

Abstract. As a low computational complexity detection algorithm for Massive Multi-Input-Multi-Output (MIMO) system, the well known factor graph belief propagation (BP) detection algorithm is effective for binary phase shift keying (BPSK) signal, but not appropriate for quadrature amplitude modulation (QAM) signal. In this paper, the complex transmitted signal vector modulated by QAM is transformed into the real valued bitwise vector which can be viewed as a transmitting signal vector modulated by BPSK. With the real valued bitwise vector and transformed channel gain matrix, an improved bitwise factor graph (BFG) graphic model is developed, and a BFG-BP algorithm is proposed to detect QAM signals in Massive MIMO system. Over a finite time of polynomial computational complexity of $O(N_T)$ per symbol, where N_T denotes the number of transmitted antennas, the proposed BFG-BP detection algorithm obtains the approximate optimum BER performance of maximum likelihood detection algorithm with rapid convergence rate, and also achieves the theoretical spectral efficiency at medium high average received signal-to-noise ratio. Simulation results prove the effectiveness of the proposed BFG-BP for detecting QAM signals in Massive MIMO system.

Keywords: Massive MIMO · Detection algorithm · Bitwise factor graph · Belief propagation · Bit error rate (BER) · Computational complexity

1 Introduction

The detection algorithm for Massive Multi Input Multi Output (MIMO) system captured much attention in recent years [1, 2]. Due to the large scale antennas in Massive MIMO system, the problem of obtaining optimum bit error rate (BER)

W. Meng—This work is supported by National Natural Science Foundation of China: No. 61471143.

along with lower computational complexity is non-deterministic polynomial-time hard (NP-hard), and is difficult to be solved.

The maximum likelihood (ML) detection algorithm obtains the optimum BER performance for MIMO system [3]. However, the computational complexity of ML increases exponentially with the number of transmitting antennas, which is too high for ML to be employed in Massive MIMO system. The traditional linear detection algorithms, such as minimum mean square error (MMSE), have much lower polynomial computational complexity than ML. But the BER performance of MMSE is poor, and is required to be improved for Massive MIMO system.

Recently, many detection algorithms for Massive MIMO system have been investigated, such as the likelihood ascent search (LAS) algorithm [4], the Markov Chain Monte Carlo (MCMC) algorithm [5], the Probabilistic Data Association (PDA) algorithm [6], the Markov random field (MRF) and the factor graph (FG) based belief propagation (BP) detection algorithms [7, 8], etc. They obtain approximate optimum BER performance with polynomial computational complexity. Particularly, the FG-BP detection algorithm has a relative low computational complexity, and has a considerable potential of application in Massive MIMO system. Though the FG-BP is effective for Binary Phase Shift Keying (BPSK) signals, it is not appropriate for quadrature amplitude modulation (QAM) signals.

In this paper, the complex transmitted signal vector modulated by QAM is transformed into the real valued bitwise vector which can be viewed as a transmitting signal vector modulated by BPSK. With the real valued bitwise vector and transformed channel gain matrix, we develop an improved bitwise factor graph (BFG) graphic model, and propose a novel BFG-BP algorithm to detect QAM signals in Massive MIMO system. With one order polynomial computational complexity, the proposed BFG-BP obtains an approximate optimum BER performance of ML, and achieves the theory spectral efficiency at a medium high average received signal-to-noise (SNR) as well.

The rest of the paper is organized as follows. The detection model for Massive MIMO system is presented in Sect. 2. Section 3 deduces the proposed BFG-BP algorithm. Section 4 gives the corresponding computational complexity. The simulation is introduced in Sect. 5. Finally, Sect. 6 draws the conclusion.

Notation. In this paper, a vector and a matrix are represented with lowercase and uppercase boldface letters. $(\cdot)^T$, $(\cdot)^{-1}$, $(\cdot)^H$, $\|\cdot\|$, \otimes , $E\{\cdot\}$, $\Re(\cdot)$ and $\Im(\cdot)$ denote transpose, inverse, complex conjugate transpose, 2-norm, Kronecker product, statistical expectation, real part and imaginary part of a matrix, respectively. \mathbb{C} and \mathbb{R} refer to the complex and real domain, respectively.

2 System Model

For both the point to point and the up-link multiuser Massive MIMO system in single cell or non-cooperative multi cell, we employ the vertical Bell Layered

space-time (VBLAST) system as the uncoded detection model [10]. For the Massive MIMO system, hundreds and thousands of antennas are considered, and the number of transmitted and received antennas are denoted as N_T and N_R , respectively. The channel gain matrix can be written as

$$\mathbf{H}' = \begin{bmatrix} h'_{11} & h'_{12} & \cdots & h'_{1N_T} \\ h'_{21} & h'_{22} & \cdots & h'_{2N_T} \\ \vdots & \vdots & \ddots & \vdots \\ h'_{N_R1} & h'_{N_R2} & \cdots & h'_{N_RN_T} \end{bmatrix} \quad (1)$$

where $\mathbf{H}' \in \mathbb{C}^{N_R \times N_T}$ and $N_R \geq N_T$. h'_{ln} denotes the channel gain from the n th transmitted antenna to the l th received antenna, $l \in \{1, 2, \dots, N_R\}$, $n \in \{1, 2, \dots, N_T\}$. In quasi-static environment, the channel is assumed to be flat fading. \mathbf{H}' is invariant during a frame, but it changes independently from frame to frame. h'_{ln} is a zero mean, independent, and identically distributed complex Gaussian random variable with variance 1. In addition, the channel state is assumed to be known at the receiver.

During a symbol time, the $N_T \times 1$ transmitted signal vector can be denoted as

$$\mathbf{x}' = [x'_1, \dots, x'_n, \dots, x'_{N_T}]^T \quad (2)$$

where $x'_n \in \mathbb{S}$ is modulated from bits stream into a symbol according to the modulation alphabet. $\mathbb{S} = \mathbb{A} + j\mathbb{A}$ is referred to as the complex alphabet of M-QAM modulation, and

$$\mathbb{A} = [-(\sqrt{M} - 1), \dots, -3, -1, 1, 3, \dots, (\sqrt{M} - 1)] \quad (3)$$

where M denotes the modulation order.

The received signal can be denoted as $\mathbf{y}' = [y'_1, \dots, y'_l, \dots, y'_{N_R}]^T \in \mathbb{C}^{N_R \times 1}$, and is given by

$$\mathbf{y}' = \mathbf{H}'\mathbf{x}' + \mathbf{w}' \quad (4)$$

where $\mathbf{w}' = [w'_1, \dots, w'_l, \dots, w'_{N_R}]^T \in \mathbb{C}^{N_R \times 1}$ refers to the complex additive white Gaussian noise (AWGN), and $E \{ \mathbf{w}'\mathbf{w}'^H \} = \sigma^2 \mathbf{I}_{N_R}$. The σ^2 is the noise variance, and \mathbf{I}_{N_R} signifies a $N_R \times N_R$ identity matrix.

3 Proposed BFG-BP Detection Algorithm

Consider the real-valued system model corresponding to (4), i.e.,

$$\mathbf{y} = \mathbf{H}\mathbf{x} + \mathbf{w} \quad (5)$$

where

$$\mathbf{y} \triangleq \begin{bmatrix} \Re(\mathbf{y}') \\ \Im(\mathbf{y}') \end{bmatrix}, \mathbf{H} \triangleq \begin{bmatrix} \Re(\mathbf{H}') & -\Im(\mathbf{H}') \\ \Im(\mathbf{H}') & \Re(\mathbf{H}') \end{bmatrix}, \mathbf{x} \triangleq \begin{bmatrix} \Re(\mathbf{x}') \\ \Im(\mathbf{x}') \end{bmatrix}, \mathbf{w} \triangleq \begin{bmatrix} \Re(\mathbf{w}') \\ \Im(\mathbf{w}') \end{bmatrix}. \quad (6)$$

Herein, \mathbf{y} , \mathbf{H} , \mathbf{x} and \mathbf{w} signify the real valued received signal vector, channel gain matrix, transmitted signal vector and noise vector, respectively. For the sake of convenience, \mathbf{y} , \mathbf{x} and \mathbf{w} are rewritten as follows:

$$\mathbf{y} = [y_1, \dots, y_{n_r}, \dots, y_{2N_R}]^T \tag{7}$$

$$\mathbf{x} = [x_1, \dots, x_{n_t}, \dots, x_{2N_T}]^T \tag{8}$$

$$\mathbf{w} = [w_1, \dots, w_{n_r}, \dots, w_{2N_R}]^T \tag{9}$$

where $n_t = 1, 2, \dots, 2N_T$, $n_r = 1, 2, \dots, 2N_R$.

In the context of M-QAM, the real valued symbol x_{n_t} is expanded to the bit domain and written as

$$x_{n_t} = \sum_{k=0}^{K-1} 2^k b_{n_t}^k = \mathbf{c} \mathbf{b}_{n_t} \tag{10}$$

where $K = \log_2(\sqrt{M})$ refers to the total number of bits for each real valued symbol, and

$$\mathbf{c} = [2^0, 2^1, \dots, 2^k, \dots, 2^{K-1}] \tag{11}$$

$$\mathbf{b}_{n_t} = [b_{n_t}^{(0)}, b_{n_t}^{(1)}, \dots, b_{n_t}^{(k)}, \dots, b_{n_t}^{(K-1)}]^T \tag{12}$$

where \mathbf{b}_{n_t} can be interpreted as the n_t th bitwise transmitted vector. $b_{n_t}^{(k)} \in \mathbb{B}$ represents the k th bit value from the n_t th transmitted antenna. $\mathbb{B} = \{1, -1\}$ signifies the bitwise alphabet. $k = 0, 1, \dots, K - 1$.

Denote

$$\mathbf{b} = [\mathbf{b}_1^T, \mathbf{b}_2^T, \dots, \mathbf{b}_{n_t}^T, \dots, \mathbf{b}_{2N_T}^T]^T \tag{13}$$

as a collection of the bitwise transmitted vector. According to (8) and (10), the transmitted signal vector \mathbf{x} can be rewritten as

$$\mathbf{x} = (\mathbf{I}_{2N_T} \otimes \mathbf{c})\mathbf{b}. \tag{14}$$

It follows from (5) and (14) that

$$\mathbf{y} = \mathbf{H}(\mathbf{I}_{2N_T} \otimes \mathbf{c})\mathbf{b} + \mathbf{w} = \tilde{\mathbf{H}}\mathbf{b} + \mathbf{w} \tag{15}$$

where $\tilde{\mathbf{H}} = \mathbf{H}(\mathbf{I}_{2N_T} \otimes \mathbf{c}) \in \mathbb{R}^{(2N_R) \times (2KN_T)}$ can be regarded as the equivalent channel gain matrix.

It can be seen that the bitwise alphabet \mathbb{B} is the same with the modulation alphabet of BPSK. The bitwise transmitted vector \mathbf{b} can be viewed as the signal which is modulated by BPSK.

According to (15), the maximum a posteriori probability (MAP) detection of \mathbf{b} can be given by [11]

$$\hat{b}_{n_t}^{(k)} = \arg \max_{b_{n_t}^{(k)} \in \mathbb{B}} p(b_{n_t}^{(k)} | \mathbf{y}, \tilde{\mathbf{H}}) \tag{16}$$

where $p(b_{n_t}^{(k)} | \mathbf{y}, \tilde{\mathbf{H}})$ denotes the posteriori probability (APP) of the $b_{n_t}^{(k)}$. According to the above derivation, we develop a bitwise FG (BFG) graphic model. Its modeling process is illustrated in Fig. 1(a).

Based on the BFG graphic model, a novel BFG-BP detection algorithm is proposed. Figure 1(b) and (c) briefly shows message passing of the proposed BFG-BP, where the observation node and the bitwise variable node signify the real valued received symbol and transmitted bit, respectively.

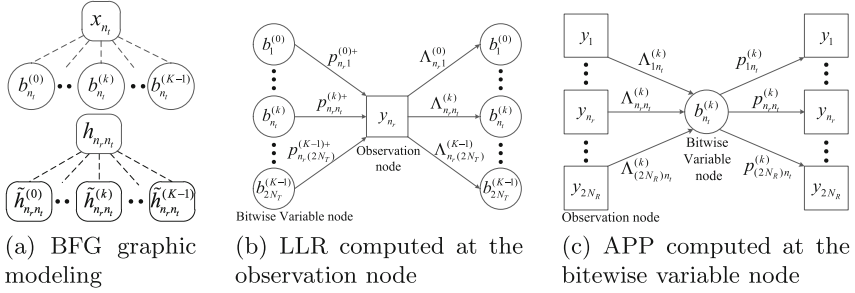


Fig. 1. Graphic modeling and message passing of the proposed BFG-BP

Consider the message which passes from the $n_t^{(k)}$ th bitwise variable node to the n_r th observation node. It follows from (7) and (15) that

$$y_{n_r} = \tilde{h}_{n_r, n_t}^{(k)} b_{n_t}^{(k)} + \sum_{j=1, j \neq n_t}^{2N_T} \sum_{i=0, i \neq k}^{K-1} \tilde{h}_{n_r, j}^{(i)} b_j^{(i)} + w_{n_r} = \tilde{h}_{n_r, n_t}^{(k)} b_{n_t}^{(k)} + z_{n_r, n_t}^{(k)} \quad (17)$$

where $\tilde{h}_{n_r, n_t}^{(k)}$ denotes the $(n_r, n_t^{(k)})$ th entry of $\tilde{\mathbf{H}}$, and

$$z_{n_r, n_t}^{(k)} = \sum_{j=1, j \neq n_t}^{2N_T} \sum_{i=0, i \neq k}^{K-1} \tilde{h}_{n_r, j}^{(i)} b_j^{(i)} + w_{n_r} \quad (18)$$

represents the Gaussian approximate interference (GAI) to the bit variable $b_{n_t}^{(k)}$, which is coming from the $n_t^{(k)}$ transmitted bitwise node and received by the n_r th observation node. In addition, $z_{n_r, n_t}^{(k)}$ approximately follows the Gaussian distribution [9], i.e., $z_{n_r, n_t}^{(k)} \sim \mathcal{CN}(\mu_{z_{n_r, n_t}^{(k)}}, \sigma_{z_{n_r, n_t}^{(k)}}^2)$, where

$$\mu_{z_{n_r, n_t}^{(k)}} = \sum_{j=1, j \neq n_t}^{2N_T} \sum_{i=0, i \neq k}^{K-1} \tilde{h}_{n_r, j}^{(i)} \mathbb{E}(b_j^{(i)}) \quad (19)$$

$$\sigma_{z_{n_r, n_t}^{(k)}}^2 = \sum_{j=1, j \neq n_t}^{2N_T} \sum_{i=0, i \neq k}^{K-1} (\tilde{h}_{n_r, j}^{(i)})^2 \text{Var}(b_j^{(i)}) + \sigma^2/2. \quad (20)$$

$\mathbb{E}(b_j^{(i)})$ and $\text{Var}(b_j^{(i)})$ denote the mean and variance of the bitwise variable $b_j^{(i)}$, respectively.

The log-likelihood ratio (LLR) of $b_j^{(i)}$ at the n_r th observation node is denoted by $\Lambda_{n_r n_t}^{(k)}$, and can be written as

$$\Lambda_{n_r n_t}^{(k)} = \log \frac{p(y_{n_r} | \tilde{\mathbf{H}}, b_{n_t}^{(k)} = +1)}{p(y_{n_r} | \tilde{\mathbf{H}}, b_{n_t}^{(k)} = -1)} = \frac{2}{\sigma_{z_{n_r n_t}}^2} \tilde{h}_{n_r n_t}^{(k)} (y_{n_r} - \mu_{z_{n_r n_t}}^{(k)}). \quad (21)$$

After passing the message of LLR from observation nodes to the $n_t^{(k)}$ th bit-wise variable node, the posterior probability of $\{b_{n_t}^{(k)} = +1\}$ is denoted by $p_{n_r n_t}^{(k)+}$, and computed as

$$p_{n_r n_t}^{(k)+} \triangleq p_{n_r n_t}^{(k)}(b_{n_t}^{(k)} = +1 | \mathbf{y}) = \frac{\exp(\sum_{m=1, m \neq n_r}^{2N_R} \Lambda_{m n_t}^{(k)})}{1 + \exp(\sum_{m=1, m \neq n_r}^{2N_R} \Lambda_{m n_t}^{(k)})}. \quad (22)$$

After a certain number of iterations, $b_{n_t}^{(k)}$ is detected as the one which has the sign of the sum of LLR for all the receiving antennas, i.e.,

$$\hat{b}_{n_t}^{(k)} = \text{sign} \left(\sum_{n_r=1}^{2N_R} \Lambda_{n_r n_t}^{(k)} \right). \quad (23)$$

4 Computational Complexity Analysis

As shown in Table 1, the computational complexity of the proposed BFG-BP detection algorithm mainly comes from three parts. Firstly, the LLR computation at the observation node given in (21) requires roughly $O(N^2)$. Secondly, the posterior probability computation at the bitwise variable node given in (22) takes about $O(N^2)$. Finally, the BFG graphic modeling described in (15) requires nearly $O(N)$. Considering that there exists N transmitted symbols, the total computational complexity of the proposed BFG-BP algorithm for each symbol is $O(N^2 + N^2 + N)/N \approx O(N)$.

Table 1. The computational complexity of the proposed BFG-BP detection algorithm

Main computational part	Computational complexity
LLR calculation	$O(N^2)$
APP calculation	$O(N^2)$
BFG graphic modeling	$O(N)$

5 Simulation Results

In the simulations, $N_T \times N_R$ is used to denote the number of transmitting and receiving antennas of the Massive MIMO system, where N_T and N_R are varied from 64 to 1024, unless otherwise stated. In addition, the detection of M-QAM signals is investigated to examine the advantages of the proposed BFG-BP detection algorithm, and $M = 4$. The average received SNR (dB) per received antenna ranges from 0 dB to 12 dB.

5.1 BER

In this simulation, the BER performance of the proposed BFG-BP detection algorithm is compared with that of the MMSE in [4]. Due to the high computational complexity of ML in Massive MIMO system, the single-input-single-output (SISO) AWGN performance is employed as a lower bound to evaluate our detection performance, where the theory BER for M-QAM of SISO AWGN is given by [12]

$$P_{theory} = a \cdot Q\left(\sqrt{b \cdot (\text{SNR}/\log_2(M))}\right) \quad (24)$$

where $a = 2(1 - 1/\sqrt{M})/\log_2(\sqrt{M})$, $b = (6\log_2(\sqrt{M})/(M - 1))$. $Q(x)$ signifies a function of x , where $Q(x) = \frac{1}{2}\text{erfc}(\frac{x}{\sqrt{2}})$ and $\text{erfc}(\cdot)$ denotes the complementary error function [12].

Figure 2(a) illustrates the BER performance of the proposed BFG-BP detection algorithm. It can be seen that when the average received SNR is 12 dB, the proposed BFG-BP reaches an average BER of 10^{-5} and approximates the BER of ML. Under the same condition, however, the MMSE only reaches an average BER of 10^{-2} . The BER of the proposed BFG-BP decreases rapidly and approximates to the optimum performance of ML, and is much better than that of MMSE, when the average received SNR increases.

Figure 2(b) shows the convergence rate of the proposed BFG-BP. In this simulation, $N_T = N_R = 128$, the average received SNR is 12 dB. The simulation result shows that the BER of the proposed BFG-BP converges to a stable scope of 10^{-5} , when the number of iteration is larger than 14. Moreover, the BER of the proposed BFG-BP reaches the optimum performance of ML.

Figure 2(c) illustrates the BER of the proposed BFG-BP versus the number of antennas. The average received SNR is fixed at 12 dB. $N_T = N_R$, and they range from 64 to 512. Evidently, the simulation result shows that the BER of the proposed BFG-BP reaches 10^{-5} , and approximates to the optimum one of ML, when N_R and N_T are larger than 64. The BER of the MMSE is roughly 10^{-2} , and almost remains unchanged even if the number of antennas goes very large. Therefore, the proposed BFG-BP is better for Massive MIMO system.

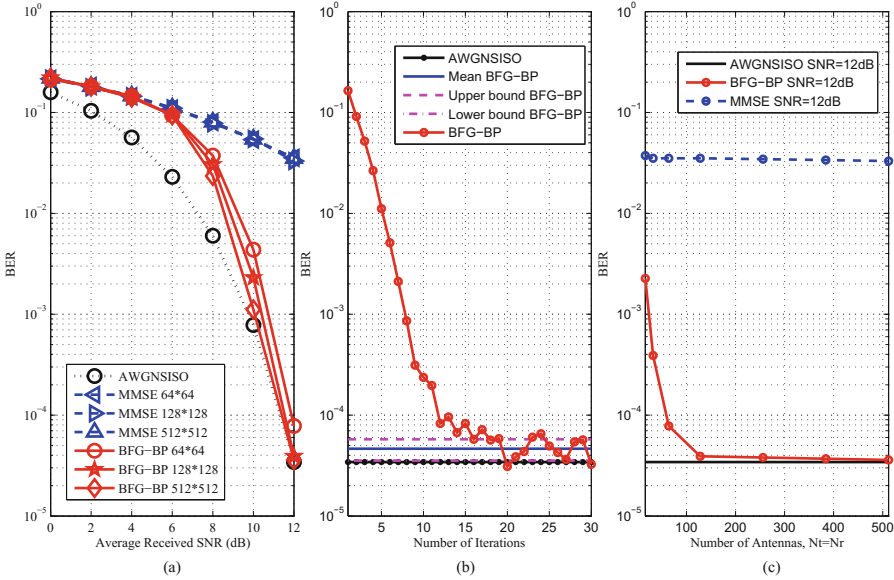


Fig. 2. The BER performance of the proposed BFG-BP detection algorithm for Massive MIMO system at 4QAM. (a) The BER versus the average received SNR (b) the convergent rate of the proposed BFG-BP, where $N_T = N_R = 128$ and the average received SNR is fixed at 12 dB (c) the BER versus the number of antennas, where $N_T = N_R$.

5.2 Spectral Efficiency

For VBLAST detection model, the theoretical spectral efficiency is denoted as SE_{theory} and given by [13]

$$SE_{theory} = N_T \log_2(M). \tag{25}$$

In the simulations, we compare the spectral efficiency of the proposed BFG-BP with the above mentioned theoretical spectral efficiency.

Figure 3(a) shows the normalized spectral efficiency per transmitted antenna of the proposed BFG-BP with the average received SNR. The results indicate that the spectral efficiency of the proposed BFG-BP increases when the average received SNR goes large, and it converges to the theoretical spectral efficiency when the average received SNR is larger than 10 dB. The least average received SNR required for the proposed BFG-BP to reach the theoretical spectral efficiency is around 12 dB, which is less than that required for MMSE.

Figure 3(b) depicts the normalized spectral efficiency per transmitted antenna of the proposed BFG-BP for increasing number of antennas, where $N_T = N_R$. It can be seen that the normalized spectral efficiency of the proposed BFG-BP increases with the number of antennas, until it converges to the normalized theory one. However, the spectral efficiency of MMSE is much lower than that of the proposed BFG-BP, and remains invariable regardless the number of antennas.

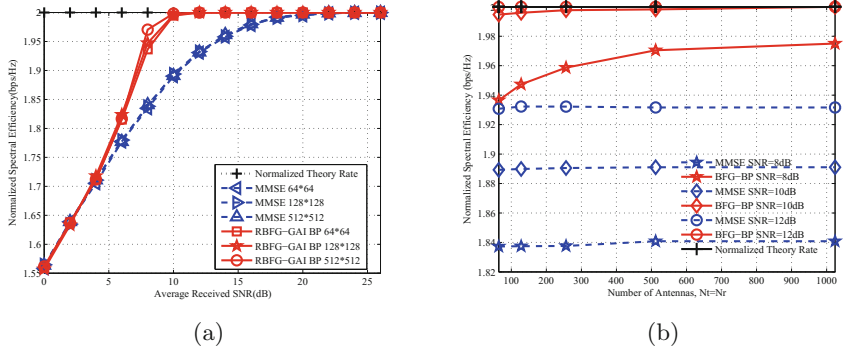


Fig. 3. The normalized spectral efficiency of Massive MIMO system by means of the proposed BFG-BP detection algorithm at 4QAM

5.3 Computational Complexity

Figure 4 illustrates the comparison of the computational complexity in the number of floating point operations (flops) among the proposed BFG-BP algorithm, the MMSE in [4] and the ML in [4]. Both BFG-BP and MMSE have a polynomially increasing computational complexity, whereas the computational complexity of ML increases exponentially with the number of antennas. Compared with MMSE and ML, the results clearly show that the computational complexity of the proposed BFG-BP is the lowest and is more applicable for Massive MIMO system.

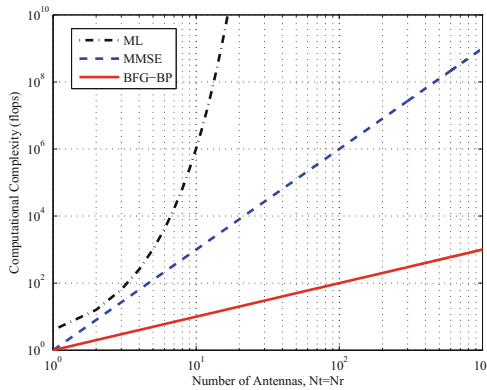


Fig. 4. The computational complexity of the proposed BFG-BP versus the number of antennas, where $N_t = N_r$.

6 Conclusion

In this paper, an improved BFG graphic model is developed, and a new BFG-BP detection algorithm is proposed for Massive MIMO system. The proposed BFG-BP detection algorithm is demonstrated to be applicable for detecting QAM signals. For Massive MIMO system, the BER performance, the spectral efficiency and the computational complexity of the proposed BFG-BP detection algorithm are better than those of the MMSE algorithm. The BER performance of the proposed BFG-BP approximates to the optimum BER of ML. The spectral efficiency of the proposed BFG-BP reaches the theoretical value, when the average received SNR is medium high or the number of transmitting and receiving antennas are large. In addition, the computational complexity of is the proposed BFG-BP is $O(N_T)$ per symbol, which increases linearly with number of antenna.

References

1. Andrews, J.G., Buzzi, S., Choi, W., et al.: What will 5G be? *IEEE J. Sel. Areas Commun.* **32**, 1065–1082 (2014)
2. Larsson, E.G., Edfors, O., Tufvesson, F., et al.: Massive MIMO for next generation wireless systems. *IEEE Commun. Mag.* **52**, 186–195 (2014)
3. Yang, S., Hanzo, L.: Fifty years of MIMO detection: the road to large-scale MIMOs. *Commun. Surv. Tutor.* **17**, 1941–1988 (2015)
4. Larsson, E.G.: MIMO detection methods: how they work. *IEEE Sig. Process. Mag.* **26**, 91–95 (2009)
5. Vardhan, K.V., Mohammed, S.K., Chockalingam, A., et al.: A low-complexity detector for large MIMO systems and multicarrier CDMA systems. *IEEE J. Sel. Areas Commun.* **26**, 473–485 (2008)
6. Chen, J., Hu, J., Sobelman, G.E.: Stochastic MIMO detector based on the Markov chain Monte Carlo algorithm. *IEEE Trans. Sig. Process.* **62**, 1454–1463 (2014)
7. Yang, S., Lv, T., Maunder, R.G., et al.: From nominal to true a posteriori probabilities: an exact Bayesian theorem based probabilistic data association approach for iterative MIMO detection and decoding. *IEEE Trans. Commun.* **61**, 2782–2793 (2013)
8. Yoon, S., Chae, C.B.: Low-complexity MIMO detection based on belief propagation over pairwise graphs. *IEEE Trans. Veh. Technol.* **63**, 2363–2377 (2014)
9. Som, P., Datta, T., Srinidhi, N., et al.: Low-complexity detection in large-dimension MIMO-ISI channels using graphical models. *IEEE J. Sel. Top. Sig. Process.* **5**, 1497–1511 (2011)
10. Loyka, S., Gagnon, F.: Performance analysis of the V-BLAST algorithm: an analytical approach. *IEEE Trans. Wirel. Commun.* **3**, 1326–1337 (2004)
11. Choi, J.: On the partial MAP detection with applications to MIMO channels. *IEEE Trans. Sig. Process.* **53**, 158–167 (2005)
12. Cho, K., Yoon, D.: On the general BER expression of one- and two-dimensional amplitude modulations. *IEEE Trans. Commun.* **50**, 1074–1080 (2002)
13. Mesleh, R.Y., Haas, H., Sinanovic, S., et al.: Spatial modulation. *IEEE Trans. Veh. Technol.* **57**, 2228–2241 (2008)